THE JOURNAL OF PHYSICAL CHEMISTRY B

Article

pubs.acs.org/JPCB

Conformational Investigation in Solution of a Fluorinated Anti-inflammatory Drug by NMR Spectroscopy in Weakly Ordering Media

Maria Enrica Di Pietro,[†,‡] Christie Aroulanda,[‡] Denis Merlet,*[,‡] Giorgio Celebre,[†] and Giuseppina De Luca*[,†]

[†]Dipartimento di Chimica e Tecnologie Chimiche, Università della Calabria, via P. Bucci, 87036, Arcavacata di Rende, Cosenza, Italy

[‡]Equipe de RMN en milieu orienté, ICMMO, UMR 8182, Université Paris-Sud, 15 Rue Georges Clemenceau, 91405 Orsay, France

Supporting Information

ABSTRACT: The structural and conformational elucidation of flexible bioactive molecules in solution is currently a crucial goal for the scientific community, but it is rarely achievable by available techniques. The anti-inflammatory drug diflunisal is presented here as a model case for supporting the efficiency of NMR spectroscopy combined with the use of weakly ordering media as a promising methodology for the conformational investigation of small bioactive molecules. Starting from NMR anisotropic data (40 independent dipolar couplings), a quite accurate description of its torsional distribution around the inter-ring C−C bond was found, characterized by a pair of two couples of conformers. According to the relative configuration of the carboxylic group and the fluorine atom in the ortho position to the inter-ring C−C bond, the more stable couple of conformers are defined as "trans" type conformers (F opposite to the carboxylic group) whereas the less stable couple are "cis" type conformers (F and carboxylic group on the same side). In order to study the influence of fluorine nuclei on the structure and conformational distribution, the same analytical strategy has been applied to investigate the phenylsalicylic acid, its nonfluorinated analogue.

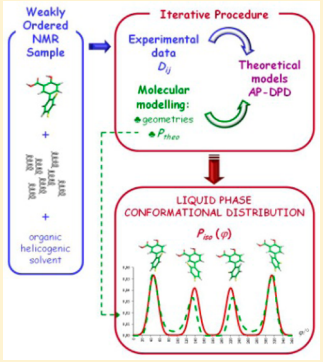

INTRODUCTION

The spatial arrangement adopted by bioactive flexible molecules strongly affects the interactions they create with endogenous ligands as well as specific systems for the controlled delivery of active agents, influencing hence their biological activity, pharmacokinetic properties, and metabolic degradation pathways.[1−3] The elucidation of three-dimensional structure and conformational equilibrium is then a preliminary step for rationalizing the relationship between conformation and drug activity and can be of valuable help for drug design, screening processes and pharmaceutical formulation development. The possibility of performing such investigation in a liquid environment is even more interesting, since it is the state of matter where molecules generally interact and, if bioactive, play their role. NMR spectroscopy satisfies both requirements. Over the years, *J*-couplings and nuclear Overhauser effect (nOe) measurements have provided clues about the conformation the drug can adopt in solution.[4] However, such standard NMR parameters are short-range in nature; thus these methods have limitations for obtaining connectivity information between atoms which are far apart and are often insufficient for an unequivocal structural and conformational determination, particularly when the measurement averages over two or more conformers.[5−7] An alternative and/or complementary strategy is the combination of NMR spectroscopy with the use of ordering liquid crystalline solvents. In such media the anisotropic part of the NMR interactions, normally averaged out to zero because of isotropic molecular tumbling, becomes readily observable. Out of the anisotropic observables—i.e., chemical shift anisotropy, anisotropy of indirect coupling, dipolar coupling, and quadrupolar splitting—dipolar couplings have been recognized to contain a unique wealth of structural, orientational, and conformational data for 1/2 spins. Thanks to their dependence on the spin−spin distances and on the orientations of the internuclear vectors with respect to the external magnetic field, these dipolar couplings represent a probe sensitive to the long-range constraints of even spatially remote parts of molecules and can thus give invaluable insights about the conformational distribution of organic compounds.[8−10] Very accurate conformational results have been reported in recent decades on small organic molecules dissolved in media such as thermotropic liquid crystals that induce a rather high degree of order.[11−16] However, the challenging spectral complexity resulting from such high order induced to the solute limited the technique to rather symmetric molecules with no more than 10 or 12 spins. Aiming at studying more complex molecules of lower symmetry, a smart choice is the use of weakly ordering solvents.[17−22] In such media anisotropic interactions are significantly reduced but not entirely averaged out to zero, allowing therefore the magnitude of dipolar couplings to be comparable to or even smaller than that of scalar couplings (this is why they are often referred to as residual dipolar couplings, RDCs). Consequently, the spectral quality of high-resolution NMR spectra is generally retained.

Received: May 23, 2014
Revised: July 4, 2014
Published: July 7, 2014

dx.doi.org/10.1021/jp505084g | *J. Phys. Chem. B* 2014, 118, 9007−9016

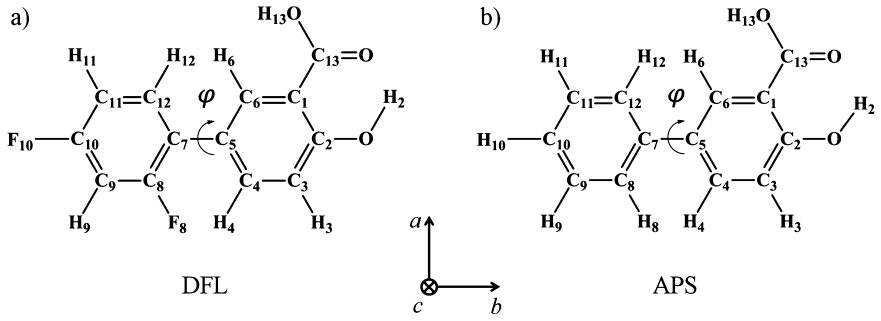

Figure 1. Topological structure, atomic labeling, and torsional angle φ of (a) diflunisal (DFL) and (b) phenylsalicylic acid (APS). The (a, b, c) axes of the molecular reference frame adopted for the molecules are also shown.

Among the several aligning media reported, those based on poly-γ-benzyl-L-glutamate (PBLG)[23] gained a wide interest. The solutions composed of the synthetic homopolypeptide PBLG (degree of polymerization higher than around 450) dissolved in helicogenic organic cosolvents (e.g , chloroform, dimethylformamide, or pyridine) create, in a magnetic field B_0 (B_0 higher than 1.4 T), chiral nematic liquid crystalline phases. A molecule dissolved therein turns out to have a low degree of orientational order: its Saupe order parameters are usually within 10^{-4} to 10^{-3}. Such ordered media were successfully used in various applications as structural and relative configuration determinations, enantiomeric excesses measurements, or discussion of reaction pathways involving a variety of organic functions and NMR isotopes.[24−34] Here we propose to apply the NMR spectroscopy in PBLG-based liquid crystalline solvents to investigate the conformational equilibrium of a nonsteroidal anti-inflammatory drug (NSAID), the 2′,4′-difluoro-4-hydroxy[1,1′-biphenyl]-3-carboxylic acid, commonly known as diflunisal (DFL, Figure 1a). DFL is a U.S. Food and Drug Administryation (FDA)-approved cyclooxygenase inhibitor, a difluorophenyl derivate of aspirin, presenting similar analgesic and anti-inflammatory therapeutic indications and side effects. Brand-name products as well as generic versions are currently available. The structural and conformational problem in complexes that DFL forms with polymeric matrices or metals as well as target proteins has been investigated in solid state by both computational techniques and X-ray, solid-state fluorescence and solid-state NMR measurements,[35−41] but to the best of our knowledge no studies have been reported on the elucidation of the molecular spatial arrangement in solution. NMR spectroscopy in ordered PBLG solutions makes it possible to explore the conformational distribution of DFL directly in a liquid medium. Note that the ability of the polypeptide fibers to readily dissolve in common low-viscosity organic solvents allows one to overcome the problem of sparing water solubility of the studied drug. As generally described, PBLG solutions have a degree of orientational order higher than other weakly orienting media, such as stretched gels.[18,19,42−51] This could be a limitation because of the possible introduction of higher-order effects in medium-sized molecules. Here, it will be an advantage, as inter-ring, long-range, dipolar couplings, which are generally small, are needed. Starting from the NMR anisotropic data, the experimental torsional distribution around the dihedral angle φ between the two rings for the DFL molecule will be investigated by using the so-called AP-DPD model and then compared with in vacuo theoretical results. The AP-DPD approach is a combination of the additive potential (AP)[52] method and the direct probability description (DPD)[53] of the conformational equilibrium. Despite being widely accepted as a robust method for describing thermotropic samples, it has been rarely used for weakly ordered solutes, so that diflunisal may represent a good test compound.

When studying the conformational features of DFL, the effect that the fluorine atoms may have on the torsional distribution is worthy of deeper investigation. Next to the interest in fundamental research, this subject has implications in drug synthesis, too. At present, the replacement of hydrogen atoms by fluorine is a well-established practice adopted by pharmaceutical chemists to obtain fluorinated compounds displaying biological activity similar to their hydrogen natural analogues but showing a greater resistance to metabolic degradation and improved bioavailability.[54−57] Indeed, though fluorine atom is still the substituent with the smallest size that can be used as replacement for hydrogen in the C−H bond in drug design, some studies suggest that the C−F bond (F van der Waals (vdW) radius = 1.47 Å) is more nearly isosteric with the C−O bond (O vdW radius = 1.52 Å) than with the C−H bond (H vdW radius = 1.20 Å).[58,59] Moreover, because of its electronegativity, moderate size, low polarizability, and bond strength, ^{19}F can have a great influence on inter- and intramolecular forces and it is well-known that the ^{1}H to ^{19}F substitution can alter the physical properties of compounds, such as boiling points, electron density distribution, surface tension in liquids, and surface energy in solids, as well as the chemical properties, such as thermodynamic bond stability, acidity and basicity, lipophilicity, and the ability to participate in hydrogen bonding.[60,61] Interestingly, the low polarizability and the slightly larger size of ^{19}F compared with ^{1}H also have consequences for the structure and molecular dynamics of fluorinated compounds. As an example consider that the lowest energy conformer of linear hydrocarbon backbones is a zigzag conformation and possesses some conformational flexibility, whereas perfluoroalkane chains present a helical structure and are essentially rigid rodlike molecules. The explanation lies in the steric repulsion of the electronically "hard" fluorine substituents bound to carbon atoms in the relative 1,3-positions.[61] Aiming at probing whether or not the ^{19}F nuclei have significant effects on the structure and/or conformational distribution of the DFL, its nonfluorinated analogue, the 4-hydroxy[1,1′-biphenyl]-3-carboxylic acid (or phenylsalicylic acid, APS, Figure 1b) was also studied.

The aim of the present work is to obtain and compare the minimum energy conformers and the whole curves of torsional potential for the fluorinated and nonfluorinated compounds dissolved in a polypeptidic liquid crystalline solvent. As

dx.doi.org/10.1021/jp505084g | J. Phys. Chem. B 2014, 118, 9007−9016

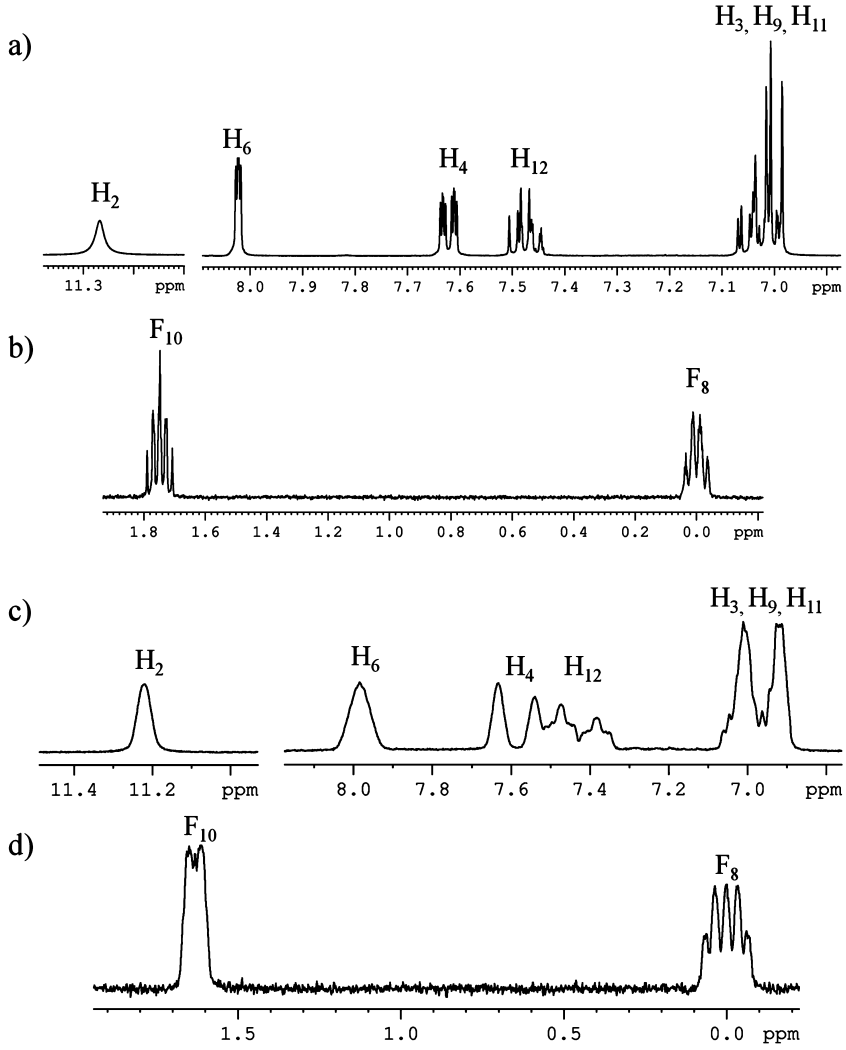

Figure 2. (a) 1D ^{1}H and (b) ^{19}F broadband excitation NMR spectra of diflunisal in tetrahydrofuran-d_8 (THF-d_8). (c) 1D ^{1}H and (d) ^{19}F broadband excitation NMR spectra of diflunisal dissolved in PBLG/THF. All NMR spectra were recorded at 9.4 T and at 300 K. In both b and d F_8 signal was arbitrarily set at 0 ppm, whereas in a and c residual ^{1}H lines of solvent were used as internal reference.

described in the following, the strategy adopted is basically a three-step operating procedure: (i) the set of experimental dipolar couplings D_{ij}^{obs} is extracted from NMR spectra; (ii) a suitable molecular geometry is obtained from molecular modeling calculations; (iii) the AP-DPD approach is applied in order to give a physical meaning to the experimental data, i.e., to obtain the conformational distribution for the studied molecules.

RESULTS AND DISCUSSION

Results from Spectral Analysis. In order to study the conformational distribution of the investigated molecules, in the first step we need the largest set of independent experimental data we can obtain, represented by the observed RDCs, D_{ij}^{obs}, between the nonequivalent *i*th and *j*th magnetically active nuclei of the molecule. Actually, what is directly measured from the anisotropic spectra is the total coupling constant defined as $|T_{ij}^{obs}| = |J_{ij}^{obs} + 2D_{ij}^{obs}|$ (for *i* and *j* nonequivalent nuclei). To be able to properly edit the set of D_{ij}^{obs}, two series of measurements are hence required: the first one on the isotropic sample, to extract the set of scalar couplings J_{ij}^{obs} (assumed basically temperature-independent), and the second one on the anisotropic sample, for measuring the total couplings T_{ij}^{obs}, to determine the targeted dipolar couplings. On both the isotropic and anisotropic samples of DFL, one-dimensional (1D) NMR ^{1}H, ^{19}F, ^{19}F−{^{1}H}, ^{13}C, ^{13}C−{^{1}H}, and ^{13}C−{^{19}F} spectra were recorded. Spectral assignment of the peaks was performed on the basis of ^{1}H−^{1}H COSY, ^{1}H−^{13}C and ^{19}F−^{13}C HSQC, and ^{1}H−^{13}C and ^{19}F−^{13}C HMBC correlation experiments. J_{ij} and T_{ij} couplings between nuclear pairs ^{1}H−^{1}H, ^{1}H−^{13}C, and ^{19}F−^{13}C were measured from experiments as two-dimensional (2D) ^{1}H−^{13}C *J*-resolved, ^{1}H−^{1}H SERF[62] and 1D ^{13}C−{^{1}H}. The extraction of J_{HF} and T_{HF} couplings, difficult to measure from broadband spectra (Figure 2) and with standard experiments, was achieved thanks to an *ad hoc* developed NMR experiment named gradient encoded heteronuclear ^{1}H−^{19}F selective refocusing (GET-SERF).[63]

A crucial point has to be noticed: only the absolute values of the indirect and total coupling constants can be measured from spectra, leading to an uncertainty concerning the signs and magnitudes of the values of the D_{ij}^{obs} to be used in the following conformational analysis. In order to reduce them, however, a strategy commonly used for getting additional analytical information in the case of one-bond ^{1}H−^{13}C dipolar couplings, $^{1}D_{CH}$, was also adopted here.[64−66] In this strategy two points

dx.doi.org/10.1021/jp505084g | J. Phys. Chem. B 2014, 118, 9007−9016

have to be recalled: (i) as the $^1J_{CH}$ scalar couplings are known to be positive,[67] the two possible $^1T_{CH}$ values derived from the $|^1T_{CH}|$ experimental value lead to only two possible $^1D_{CH}$ values; (ii) using ^2H NMR at natural abundance level, the quadrupolar splitting $\Delta\nu_{CDk}$ can be measured for the $^{13}C-^2H$ bonds. Following and combining the definitions of $^1D_{CH}$ and its corresponding $\Delta\nu_{CDk}$ for a given C−H bond, it can be demonstrated that the ratio $\Delta\nu_{CDk}/^1D_{CH}$ lies approximately in the range of −12 to −10.[68,69] Consequently, by a simple comparison of the two experimental $^1D_{CH}$ possible values with the expected one, predicted by the ratio $\Delta\nu_{CDk}/^1D_{CH}$, the correct magnitude and sign were unambiguously determined for $^1D_{CH}$. Note that the difficulties in the assignment of the quadrupolar doublets were easily overcome by recording the natural abundance deuterium (NAD) 2D autocorrelation Q-COSY[70,71] spectrum (reported in Figure 1 of the Supporting Information (SI)). Once we got a reliable starting set of dipolar couplings, the determination of the rest of the D_{ij}^{obs} was carried out, in the different fragments first and in the total molecule afterward, by a trial and error process. This means that, for each single coupling, one assumes one by one a possible value (sign and magnitude) and evaluates the consistence with the structure kept rigid and the whole set of dipolar couplings (see ref 72 and refs therein). Identical analytical procedure was also used on the isotropic and anisotropic samples of APS. From the totality of the experimental couplings, only those whose sign and value were assigned with a high level of confidence were included in the analysis, for a total of 40 independent D_{ij}^{obs} for DFL and 27 for APS (reported in Tables 1 and 2, respectively).

Molecular Modeling Calculations. The second step of the procedure for determining the conformational distribution requires molecular modeling calculations, especially the geometry of the most stable conformers and a good estimate of the potential energy surface (PES). Density functional theory (DFT) approach with the functional B3LYP and the basis set 6-31++G**, using the Gaussian09 software package,[73] was chosen. First, structures and locations of the lowest minimum energy conformers for both the DFL and APS molecules were evaluated in vacuo. In order to exclude significant solvent effects, geometry optimization calculations were also performed taking into account tetrahydrofuran as medium, by means of the polarizable continuum model (PCM)[74] implemented in the Gaussian package. No significant difference in terms of structure and relative energies of the most stable conformers emerged between the gas and liquid states. Then, assuming the bond lengths and angles are, to a good approximation, independent of the conformational state, the minimum energy structures found for an isolated molecule were used to perform for both the compounds a rigid PES scan in vacuo for the torsion angle φ between the two rings (defined as the dihedral angle $C_4-C_5-C_7-C_8$) over the 0°−360° range with a 5°-step sampling. This hypothesis of weak correlation between geometrical data and conformational distribution was carefully tested and validated in the case of DFL. Indeed, no significant difference was observed on the structures and proportions of conformers obtained by allowing a geometry optimization at each step of the conformational sampling and by the rigid PES scan described.

For DFL four minimum energy conformers were found (Figure 3a): (i) a couple of "trans" conformers with F_8 opposite to the carboxylic group (φ = ±43.2°) corresponding to the absolute minima, where the relative potential energy, E_{pot}^{rel}, is fixed to be 0 kJ/mol, and (ii) a couple of "cis" conformers with F_8 on the same side as the carboxylic group (φ = ±135.2°) corresponding to the relative minima (E_{pot}^{rel} ∼ 1.18 kJ/mol). The theoretical Boltzmann distribution can be roughly calculated from the potential energy values as

$$P_{theo}(\varphi) \propto \exp(-E_{pot}^{rel}/RT) \quad (1)$$

Table 1. Experimental Dipolar Couplings D_{ij}^{obs} Determined by the NMR Analysis of DFL Dissolved in PBLG/THF, Compared with the D_{ij}^{calc} values[a]

i	j	D_{ij}^{obs}[b] (Hz)	D_{ij}^{calc}[c] (Hz)
	C−H Couplings		
C_3	H_3	30.0 ± 0.4	30.0
C_3	H_4	−9.0 ± 0.4	−10.0
C_4	H_4	−24.9 ± 0.4	−24.8
C_4	H_6	0.5 ± 0.4	1.1
C_6	H_4	0.3 ± 0.4	0.4
C_6	H_6	31.8 ± 0.4	31.7
C_9	H_9	4.7 ± 0.4	4.4
C_9	H_{11}	0.8 ± 0.4	1.1
C_{11}	H_{11}	13.8 ± 0.4	13.8
C_{12}	H_{12}	3.7 ± 0.4	4.1
	C−F Couplings		
C_8	F_8	8.0 ± 0.5	8.3
C_8	F_{10}	−1.4 ± 0.5	−1.3
C_9	F_8	−3.1 ± 1.1	−3.4
C_9	F_{10}	−3.1 ± 1.1	−3.2
C_{10}	F_8	−0.4 ± 0.5	−0.4
C_{10}	F_{10}	−32.7 ± 0.5	−32.5
C_{12}	F_8	0.9 ± 0.5	0.9
C_{12}	F_{10}	−1.5 ± 0.5	−1.5
	H−H Couplings		
H_3	H_4	−22.5 ± 0.3	−23.0
H_3	H_6	2.0 ± 0.3	1.3
H_4	H_6	1.4 ± 0.2	1.7
H_4	H_9	−1.5 ± 0.3	−1.1
H_4	H_{11}	−1.5 ± 0.3	−1.0
H_4	H_{12}	−2.5 ± 0.2	−2.3
H_6	H_9	−2.3 ± 0.3	−2.4
H_6	H_{11}	−2.3 ± 0.3	−2.2
H_6	H_{12}	−5.1 ± 0.2	−5.4
H_9	H_{11}	2.3 ± 0.2	2.2
H_{11}	H_{12}	−22.2 ± 0.3	−22.1
	H−F Couplings		
H_4	F_8	−0.9 ± 0.3	−0.7
H_4	F_{10}	−1.1 ± 0.5	−0.7
H_6	F_8	−6.3 ± 0.3	−6.6
H_6	F_{10}	−2.0 ± 0.5	−1.6
H_9	F_8	−18.9 ± 0.3	−18.3
H_9	F_{10}	2.7 ± 0.3	2.1
H_{11}	F_8	0.5 ± 0.3	0.5
H_{11}	F_{10}	−0.6 ± 0.3	−1.0
H_{12}	F_8	1.9 ± 0.3	1.8
H_{12}	F_{10}	−2.3 ± 0.3	−2.6
	F−F Couplings		
F_8	F_{10}	−1.6 ± 0.3	−1.5
RMS		0.31 Hz	

[a]Good agreement implies a small RMS value. [b]Calculated from $D_{ij}^{obs} = (T_{ij}^{obs} - J_{ij}^{obs})/2$. [c]From the AP-DPD method.

dx.doi.org/10.1021/jp505084g | J. Phys. Chem. B 2014, 118, 9007−9016

Table 2. Experimental Dipolar Couplings D_{ij}^{obs} Determined by the NMR Analysis of APS Dissolved in PBLG/THF, Compared with the D_{ij}^{calc} Values[a]

i	j	D_{ij}^{obs}[b] (Hz)	D_{ij}^{calc}[c] (Hz)
	C−H Couplings		
C_1	H_3	0.7 ± 0.5	0.7
C_1	H_4	−1.0 ± 0.5	−0.5
C_3	H_3	25.9 ± 0.5	25.6
C_3	H_4	−5.8 ± 0.5	−5.7
C_4	H_4	−21.3 ± 0.5	−21.3
C_4	H_6	0.6 ± 0.5	0.7
C_6	H_3	0.6 ± 0.6	0.6
C_6	H_4	0.2 ± 0.5	0.1
C_6	H_6	25.6 ± 0.5	25.9
C_8	H_8	16.5 ± 0.5	16.8
C_9	H_9	16.9 ± 0.5	16.7
C_{10}	H_9	4.1 ± 0.5	4.0
C_{10}	H_{10}	−29.3 ± 0.5	−30.0
C_{10}	H_{11}	4.1 ± 0.5	4.0
C_{11}	H_{11}	16.9 ± 0.5	16.7
C_{13}	H_6	−2.3 ± 0.5	−2.3
	H−H Couplings		
H_3	H_4	−10.7 ± 0.3	−10.0
H_3	H_6	1.4 ± 0.3	1.1
H_4	H_6	1.1 ± 0.3	0.8
H_4	H_8	−2.1 ± 0.3	−2.1
H_4	H_{12}	−2.1 ± 0.3	−2.1
H_6	H_8	−5.7 ± 0.3	−5.7
H_6	H_9	−1.6 ± 0.4	−1.2
H_6	H_{10}	−1.5 ± 0.4	−1.0
H_6	H_{11}	−1.6 ± 0.4	−1.2
H_6	H_{12}	−5.7 ± 0.3	−5.7
H_8	H_9	−10.8 ± 0.4	−10.2
H_8	H_{10}	−0.6 ± 0.4	−0.9
H_8	H_{11}	0.9 ± 0.4	0.7
H_8	H_{12}	2.2 ± 0.4	2.0
H_9	H_{10}	5.3 ± 0.4	5.3
H_9	H_{11}	2.3 ± 0.4	2.0
H_9	H_{12}	0.9 ± 0.4	0.7
H_{10}	H_{11}	5.3 ± 0.4	5.3
H_{10}	H_{12}	−0.6 ± 0.4	−0.9
H_{11}	H_{12}	−10.8 ± 0.4	−10.2
RMS		0.35 Hz	

[a]Good agreement implies a small RMS value. [b]Calculated from $D_{ij}^{obs} = (T_{ij}^{obs} - J_{ij}^{obs})/2$. [c]From the AP-DPD method.

where T denotes the absolute temperature and R the universal gas constant. From eq 1 relative percentages of 30% for each trans conformer and 20% of each cis conformer were calculated.

In the case of APS, as expected for symmetry reasons, four equally probable minimum energy conformers resulted from the molecular modeling calculations (Figure 3b). Torsion angle values of the conformers are respectively $\varphi = \pm 39.1°$ and $180° \pm 39.1°$. From a purely geometrical viewpoint it is reasonable that the replacement $^1H-^{19}F$ in APS with respect to DFL affects some bond lengths and angles. For a direct comparison we report in the SI (Table 1) the optimized geometries of the minimum energy conformers found for DFL and APS. Besides the trivial difference in the length of the C−F bonds (~1.36 Å) compared to the corresponding C−H bonds (~1.086 Å), it is interesting to note that the presence of protons instead of

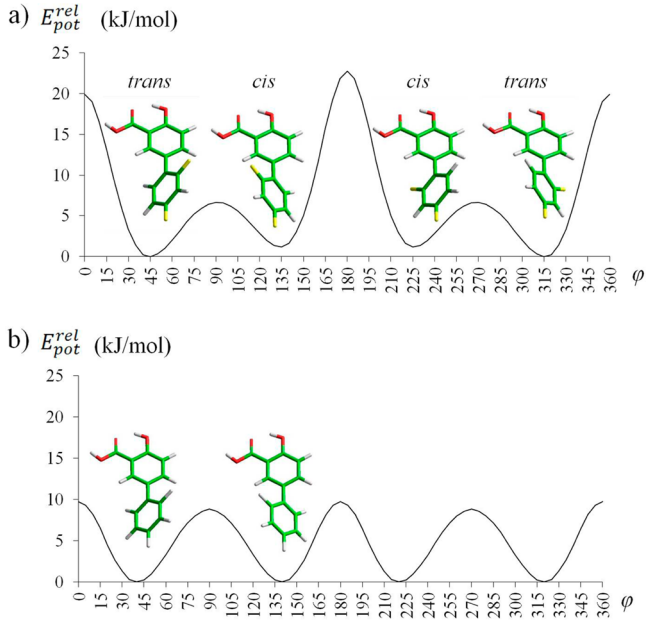

Figure 3. Relative potential energy as a function of $\varphi = C_4C_5C_7C_8$ obtained from B3LYP/6-31++G** calculations in vacuo for (a) DFL and (b) APS, including structures of the corresponding minimum energy conformers.

fluorine atoms in the APS molecule affects almost all internal angles of the corresponding ring as well as angles between the inter-ring C_5-C_7 bond and each phenyl ring.

Conformational Analysis. To extract the desired conformational information from the experimental dipolar couplings, it is necessary to invoke a model taking into account the variation of the orientational order with the conformational state. In this work, within a mean field approach, the so-called AP-DPD model, a combination of the additive potential model[52] for the treatment of the ordering interactions with the direct probability description[53] of the torsional distribution $P_{iso}(\{\phi\})$, was used. In the following, the AP-DPD approach is shortly described (for an extensive rigorous theoretical description see refs 11 and 75).

For a flexible molecule, the observed dipolar couplings result from an average over all the ϕ conformations and can be approximated to

$$D_{ij}^{obs} \approx \frac{2}{3}\frac{Z_{iso}}{Z}\left(\frac{3\cos^2\omega - 1}{2}\right)\int P_{iso}(\{\phi\})\, Z_{ext}(\{\phi\}) \times \sum_{\alpha\beta} S_{\alpha\beta}(\{\phi\})\, D_{ij,\alpha\beta}(\{\phi\})\, d\{\phi\} \quad (2)$$

where ω is the angle between the external magnetic field B_0, defining the Z direction in the laboratory frame, and $\hat{n}$, the director of the mesophase; $\{\phi\}$ is the set of internal angles defining the conformation. Z, Z_{iso}, and $Z_{ext}(\{\phi\})$ are proper normalization factors, and the term $P_{iso}(\{\phi\})$ defines the probability distribution of the solute in a conventional isotropic liquid sharing, at the experimental temperature, the same physical properties of the liquid-crystalline solvent, with the exception of its ability to induce a solute ordering. Hence, it must be stressed here that $P_{iso}(\{\phi\})$ is definitely the pertinent conformational target. The terms $S_{\alpha\beta}(\{\phi\})$ are the solute orientational order parameters, constituting the real symmetric traceless Saupe ordering matrix, and the $D_{ij,\alpha\beta}(\{\phi\})$ are the

dx.doi.org/10.1021/jp505084g | J. Phys. Chem. B 2014, 118, 9007−9016

Cartesian components, given in the molecular frame, of the D_{ij} dipolar coupling tensor between the ith and the jth nuclei.[75]

The main consequence of eq 2 is that a theoretical model describing both the conformation−orientation anisotropic interactions and $P_{iso}(\{\phi\})$ must be adopted. Within the AP model, the orientational interaction energy is described by a spherical harmonics expansion whose $\{\phi\}$-dependent coefficients can be conveniently constructed as a sum of $\{\phi\}$-independent tensorial contributions $\varepsilon^{j}_{2,p}$ from each rigid fragment j of the molecule.[76] In practice, the $\varepsilon^{j}_{2,p}$ are unknown quantities whose values are adjusted to obtain the best agreement with the experimental data. In the specific case of DFL, the treatment of the whole molecule requires six fragment tensors $\varepsilon^{j}_{2,p}$, as follows: $\varepsilon^{\text{ring A}}_{2,0}$ and $\varepsilon^{\text{ring A}}_{2,2}$ for the biaxial C_{2v}-symmetry fluorinated ring (ring A); $\varepsilon^{\text{ring B}}_{2,0}$ and $\varepsilon^{\text{ring B}}_{2,2}$, for the biaxial C_{2v}-symmetry salicylic ring (ring B); $\varepsilon^{\text{C−F}}_{2,0}$ for the monoaxial component along the C_8-F_8 bond direction; $\varepsilon^{\text{C−C}}_{2,0}$, for the monoaxial component along the C_1-C_{13} bond direction. For the APS molecule the same $\varepsilon^{j}_{2,p}$ are required, with the exception of $\varepsilon^{\text{C−F}}_{2,0}$, obviously not considered, leading to a total of five tensor parameters.

The DPD approach accounts for the torsional distribution and its strength is in modeling the $P_{iso}(\{\phi\})$ in terms of Gaussian functions. For DFL and APS the presence of a hydrogen bond between -C_{13}═O and -O−H_2 reduces to one the degree of flexibility of the molecule. This means that $P_{iso}(\{\phi\})$ is equals to $P_{iso}(\varphi)$, the torsional probability distribution around the single inter-ring torsion angle φ = $C_4-C_5-C_7-C_8$. For diflunisal, $P_{iso}(\varphi)$ can be directly modeled as a sum of four Gaussian functions corresponding to the two nonequally probable couples of conformers (as anticipated by the in vacuo calculations):

$$P_{iso}(\varphi) \propto \left\{ \frac{A_1}{2}\exp\left[-\frac{(\varphi-\varphi_1^{\max})^2}{2h_1^2}\right] + \frac{A_1}{2}\exp\left[-\frac{(\varphi-\pi+\varphi_1^{\max})^2}{2h_1^2}\right] + \frac{A_2}{2}\exp\left[-\frac{\left(\varphi-\frac{\pi}{2}+\varphi_2^{\max}\right)^2}{2h_2^2}\right] + \frac{A_2}{2}\exp\left[-\frac{\left(\varphi-\frac{\pi}{2}-\varphi_2^{\max}\right)^2}{2h_2^2}\right]\right\} \quad (3)$$

where $\varphi_1^{\max}$ and $\varphi_2^{\max}$ are the most probable values of the torsion angle, A_1 and A_2 are the relative weights of the two couples (we also fixed the constraint $A_1 + A_2 = 1$), and, finally, h_1 and h_2 give the width at half-maximum height of each Gaussian.

For APS, as a consequence of the higher symmetry due to the ^1H to ^{19}F substitution, $P_{iso}(\varphi)$ can be simply derived as the sum of four equally weighted Gaussian functions:

$$P_{iso}(\varphi) \propto \left\{ \exp\left[-\frac{(\varphi-\varphi^{\max})^2}{2h^2}\right] + \exp\left[-\frac{(\varphi-\pi+\varphi^{\max})^2}{2h^2}\right] + \exp\left[-\frac{\left(\varphi-\frac{\pi}{2}+\varphi^{\max}\right)^2}{2h^2}\right] + \exp\left[-\frac{\left(\varphi-\frac{\pi}{2}-\varphi^{\max}\right)^2}{2h^2}\right]\right\} \quad (4)$$

where $\varphi^{\max}$ represents the most probable value of the torsion angle and h gives the width at half-maximum height of the Gaussians.

It is worth noting the AP model is unanimously recognized as an effective and robust method commonly applied to thermotropic systems, but there are only a few examples of application to flexible molecules dissolved in weakly orienting phases.[69,77] Therefore, the cases of DFL and APS can also be considered as test models in confirming the efficacy and robustness of the AP-DPD approach when applied to lyotropic systems.

Using the defined theoretical apparatus, the main purpose of the work, the experimental investigation of the conformational equilibrium of DFL and its comparison with that of APS, can be now addressed. Practically speaking, the determination of the conformational distribution of the molecules under investigation is obtained from the collected experimental dipolar couplings, fixing the geometry as from molecular modeling calculations, via the AP-DPD theoretical approach, through a dedicated homemade software called AnCon.[78] The calculations are carried out by fitting a set of calculated dipolar couplings (obtained by a trial set of orientational, geometrical, and potential parameters) against the experimental ones, while iterating on a pertinent number of unknowns until their optimized values. Such unknowns are (i) orientational parameters, represented by the set of the chosen $\varepsilon^{j}_{2,p}$ solute−solvent interaction tensor elements, and (ii) potential parameters, represented by the terms needed to model the conformational probability in terms of Gaussian functions (namely, the $\varphi_1^{\max}$, $\varphi_2^{\max}$, $h_1 = h_2$, and $A_1 = 1 - A_2$ terms of eq 3 and the $\varphi^{\max}$ and h terms of eq 4). At the end of the convergent process, back-calculated dipolar couplings, D_{ij}^{calc}, are carefully compared to the experimental ones. Assuming the assignment and the geometry are adequate, all differences between calculated and experimental data as well as the RMS (root-mean-square) error (RMS = $\{M^{-1}\sum_{i<j}[D_{ij}^{\text{obs}} - D_{ij}^{\text{calc}}]^2\}^{1/2}$, M being the number of independent couplings) are small. In contrast, when the calculation diverges or gives some unacceptably large differences between experimental and back-calculated data, some parameters are adjusted, in the attempt to reproduce the whole set of D_{ij}^{obs}, until an acceptable value for the RMS target function and a good agreement between D_{ij}^{obs} and D_{ij}^{calc} are reached.

In the case of DFL, 10 unknowns (6 $\varepsilon^{j}_{2,p}$ and 4 potential terms) have to be determined using 40 independent D_{ij}^{obs} (21 for the fluorinated ring, 9 for the salicylic ring, 10 between the two rings). Therefore, the problem is overdetermined from the ratio (independent target D_{ij})/(adjustable parameters) = 40/10 = 4. Then, the resolution of the system adjusting simultaneously all parameters is theoretically possible. However, because of the strong interdependence between the potential terms $\varphi_1^{\max}$, $\varphi_2^{\max}$, and A_1 with $h_1 = h_2$ and especially because of the small magnitude of the experimental D_{ij}^{obs}, the system does not converge when a simultaneous iteration on all of the unknowns is performed. As a consequence, we adjusted the different parameters of eq 3 step by step. After optimization, a good agreement between D_{ij}^{obs} and D_{ij}^{calc} has been obtained, as shown in Figure 4 and reported in the last column of Table 1.

The optimized parameters and the torsional probability $P_{iso}(\varphi)$ calculated by this approach are shown in Table 3 and in Figure 5 (solid line), respectively. $P_{iso}(\varphi)$ is characterized by a couple of trans conformers (absolute maxima), having $\varphi_1^{\max}$ = ±45.5° and a relative percentage of 56%, and a couple of cis conformers (relative maxima), having $\varphi_2^{\max}$ = ±41.1° and a relative percentage of 44%. This solution is in good agreement with molecular modeling calculations, with only small changes in the values of the probability ratio between the two couples of conformers and the torsion angles corresponding to the maxima positions. The similarity between experimental and theoretical results is straightforward to catch in Figure 5, where

dx.doi.org/10.1021/jp505084g | J. Phys. Chem. B 2014, 118, 9007−9016

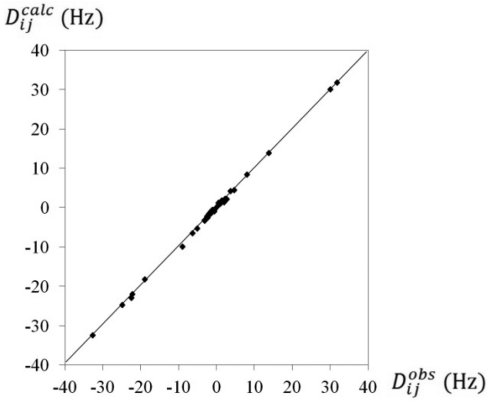

Figure 4. Observed versus theoretical dipolar couplings obtained for the DFL respectively from NMR experiments and by the AP-DPD approach.

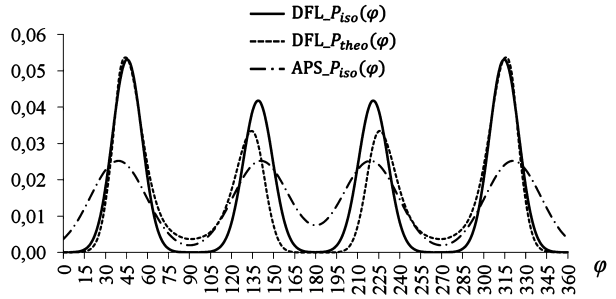

Figure 5. Comparison between the experimental torsional probability distributions obtained in PBLG/THF by the AP-DPD approach for diflunisal (solid line) and phenylsalicylic acid (dashed−dotted line) and the theoretical torsional probability distribution (dashed line) obtained for diflunisal from B3LYP/6-31++G** calculations, as a function of φ. All curves are obtained by varying φ over the 0°−360° range with a 5°-step sampling.

the theoretical probability distribution, $P_{\text{theo}}(\varphi)$, calculated from the potential energy values obtained by DFT calculations is plotted (dashed line) together with the experimental $P_{\text{iso}}(\varphi)$.

For the nonfluorinated molecule, both the amount of target dipolar couplings and adjustable parameters are reduced with respect to DFL: there are 27 independent experimentally collected D_{ij}^{obs}, 10 for the unsubstituted ring, 13 for the salicylic ring, and only 4 between the two rings, and 7 unknowns to be determined, 5 $\varepsilon_{2,p}^{i}$ and 2 potential terms, $\varphi^{\max}$ and h. Calculations were performed by varying $\varphi^{\max}$, with a parametrical adjustment of h. The best fit between D_{ij}^{obs} and D_{ij}^{calc}, reported in Table 2 and shown in Figure 6, was reached for the optimized parameters reported in Table 3, corresponding to the $P_{\text{iso}}(\varphi)$ shown in Figure 5 (dashed−dotted line), characterized by four equally probable conformers having $\varphi^{\max} = \pm 40°$ and $180° \pm 40°$. This result is evidently in agreement with the values obtained for an isolated molecule by the DFT calculation.

A comparison between the conformational probability distributions $P_{\text{iso}}(\varphi)$ reported in Figure 5 for the fluorinated DFL (solid line) and nonfluorinated APS (dashed−dotted line) molecules in liquid-like solvent immediately reveals two main differences, in the exact position of the maxima and in the width of the Gaussian functions. First, the inter-ring torsion angles found for the most stable conformers of APS are slightly smaller than those that resulted in the analysis of DFL (about 3° between the average $(\varphi_1^{\max} + \varphi_2^{\max})/2$ in DFL and $\varphi^{\max}$ in

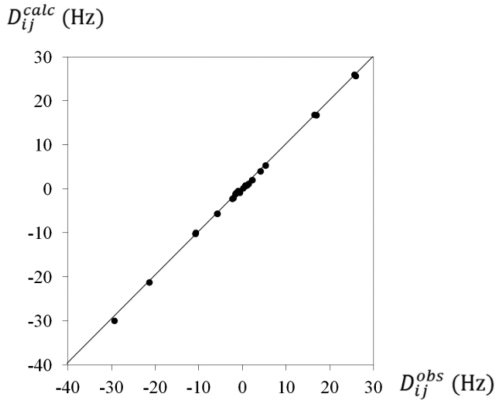

Figure 6. Observed versus theoretical dipolar couplings obtained for APS respectively from NMR experiments and by the AP-DPD approach.

APS). This result could be merely associated with the greater van der Waals radius of the fluorine nucleus compared to the proton,[79] implying a weak steric hindrance effect in the rotation around the C_5-C_7 bond in the case of APS. A similar result for instance was found from B3LYP/6-311+G* in vacuo theoretical calculations performed on 2-halogen-substituted biphenyls, where the presence of fluorine was demonstrated to have a much smaller influence on the φ value compared to other halogens.[80] The optimized twist angle was found to be of

Table 3. Optimized Values of the Iteration Parameters Used in the Conformational Analysis with the AP-DPD Approach of the DFL and APS Molecules Dissolved in PBLG/THF

parameter	DFL	parameter	APS
$\varphi_1^{\max}$/deg	45.5 ± 2.1	$\varphi^{\max}$/deg	40 ± 15
$\varphi_2^{\max}$/deg	41.1 ± 1.2	h/deg	27.5 ± 2.5[a]
$h_1 = h_2$/deg	10.5 ± 1.8	$\varepsilon_{2,0}^{\text{ring A}}/RT$	−0.005 ± 0.002
A_1	0.56 ± 0.02	$\varepsilon_{2,2}^{\text{ring A}}/RT$	−0.0152 ± 0.0009
$\varepsilon_{2,0}^{\text{ring A}}/RT$	−0.03 ± 0.01	$\varepsilon_{2,0}^{\text{ring A}}/RT$	0.009 ± 0.002
$\varepsilon_{2,2}^{\text{ring A}}/RT$	−0.02 ± 0.01	$\varepsilon_{2,2}^{\text{ring B}}/RT$	−0.0014 ± 0.0008
$\varepsilon_{2,0}^{\text{C−F}}/RT$	−0.00040 ± 0.00001	$\varepsilon_{2,0}^{\text{C−C}}/RT$	0.0064 ± 0.0002
$\varepsilon_{2,0}^{\text{ring B}}/RT$	0.04 ± 0.01	RMS/Hz	0.31
$\varepsilon_{2,2}^{\text{ring B}}/RT$	−0.018 ± 0.005		
$\varepsilon_{2,0}^{\text{C−C}}/RT$	0.0087 ± 0.0005		
RMS/Hz	0.35		

[a]After parametrization.

dx.doi.org/10.1021/jp505084g | J. Phys. Chem. B 2014, 118, 9007−9016

42.5°, 45.1°, and 59.9° for biphenyl, 2-fluorobiphenyl, and 2-chlorobiphenyl, respectively. Indeed, if one looks at the error associated with the φ^{max} value in APS (Table 3), it is evident that the torsion angle value can cover a large range, including the φ_1^{max} and φ_2^{max} values found for DFL. The second difference observed in Figure 5 is that the peaks characterizing the $P_{iso}(\varphi)$ distribution of APS appear less sharp than those obtained for the DFL. The sharpness of the peaks is related to the magnitude of the parameter h, which was found out of 10.5 ± 1.8° and 27.5 ± 2.5° for DFL and APS, respectively. From a physical point of view, this would suggest a difference in the torsional barriers for the fluorinated and nonfluorinated compounds. In other words the presence of ^{19}F nuclei would make DFL be more confined in proximity of its conformational minima with respect to APS.

EXPERIMENTAL SECTION

Sample Preparation and NMR Experiments. Two isotropic solutions were obtained by diluting DFL (30 mg) in THF-d_8 (483 mg) and APS (23 mg) in THF-d_8 (490 mg). The anisotropic samples were prepared by dissolving DFL (33 mg) in a liquid-crystalline phase made of PBLG (82 mg, DP = 743) and THF (474 mg) and phenylsalicylic acid (27 mg) in a liquid-crystalline phase composed of PBLG (484.5 mg, DP = 743) and THF (84 mg). All anisotropic samples were prepared using a standard procedure described in literature,[64] and the resulting 5 mm o.d. NMR tubes were centrifuged back and forth until an optically homogeneous birefringent phase was obtained. DFL, APS, THF, and PBLG were purchased from Sigma-Aldrich, while THF-d_8 was from Eurisotop. All of the chemical compounds were used without further purification.

All of the ^1H, ^{19}F, and ^{13}C spectra were recorded at 300 K on a liquid high-resolution Bruker Avance 400 MHz spectrometer (9.4 T) equipped with a BBI or QXO probe with a z field-gradient coil. The ^{19}F lock channel of the QXO probe was used for the fluorine pulses. The NAD spectra were recorded on a high-resolution Bruker Avance II 600 MHz spectrometer (14.1 T) equipped with a 5 mm selective ^2H cryoprobe. Temperature was carefully fed back at 300 K by a standard variable-temperature unit (BVT-3000). All the spectral parameters extracted for DFL and APS are reported in Tables 2, 3, and 4 of the SI.

CONCLUSION

The structure and conformational equilibrium of the fluorinated anti-inflammatory drug diflunisal have been investigated by NMR spectroscopy in weakly ordering liquid crystals. For the first time the whole curve of torsional potential of a small compound dissolved in low-ordering anisotropic solvent has been experimentally determined, and it turns out to be in agreement with theoretical calculations at the DFT level. The probability distribution of the solute shows a couple of trans conformers with $\varphi_1^{max} = \pm 45.5°$ and relative percentage of 56% and a couple of cis conformers with $\varphi_2^{max} = \pm 41.1°$ and a relative percentage of 44%. In order to probe the influence the fluorine nuclei have on the conformational equilibrium of the diflunisal, its nonfluorinated analogue, phenylsalicylic acid, has been studied under similar conditions. Results seem to suggest a smoothing in the torsional barriers. The investigated compounds represent a good test for the robustness of the AP-DPD approach that proves to be a reliable method to treat also weakly ordered solutes.

The study presented here supports the use of NMR spectroscopy in ordered PBLG solutions for the conformational analysis of complex bioactive flexible molecules, which are almost impossible to treat using thermotropic solvents and rarely studied in solution by other techniques. The benefit to using this anisotropic phase is to obtain long-range dipolar couplings allowing connection of the two rings. The proposed methodology can reveal thus very attractive in fields such as life science and medicinal chemistry, where the demand for detailed knowledge of the conformational repartition of pharmacologically active molecules is more and more impelling, in order to rationalize the interactions that the drug creates with the environment and consequently to explain the mechanism of action and to design new target compounds.

ASSOCIATED CONTENT

Supporting Information

Figure showing Q-COSY Fz spectrum recorded on diflunisal in PBLG/THF and tables listing optimized geometries obtained by the Gaussian09 software package (B3LYP/6-31++G**) for DFL and APS and NMR spectral parameters extracted for DFL and APS. This material is available free of charge via the Internet at http://pubs.acs.org.

AUTHOR INFORMATION

Corresponding Authors

*(D.M.) Fax: +33169158105. Tel.: +33169157432. E-mail: denis.merlet@u-psud.fr.

*(G.D.L.) Fax: +39 0984493301. Tel.: +39 0984493323. E-mail: giuseppina.deluca@unical.it.

Notes

The authors declare no competing financial interest.

ACKNOWLEDGMENTS

The present work has been supported by the European Commission, the European Social Fund, and the Regione Calabria through the cofunded Ph.D. scholarship of M.E.D.P. Moreover, G.C., G.D.L., and M.E.D.P. thank University of Calabria and MIUR PRIN 2009 for financial support.

ABBREVIATIONS

AP, additive potential; APS, phenylsalicylic acid; DFL, diflunisal; DFT, density functional theory; DPD, direct probability description; FDA, food and drug administration; GET-SERF, gradient encoded heteronuclear $^1H-^{19}F$ selective refocusing; NAD, natural abundance deuterium; NSAID, nonsteroidal anti-inflammatory drug; PBLG, poly-γ-benzyl-L-glutamate; PCM, polarizable continuum model; PES, potential energy surface; RDC, residual dipolar couplings; RMS, root-mean-square

REFERENCES

(1) Boehr, D.; Nussinov, R.; Wright, P. The Role of Dynamic Conformational Ensembles in Biomolecular Recognition. *Nat. Chem. Biol.* **2009**, *5*, 789−796.

(2) Hilt, J. Z.; Byrne, M. E. Configurational Biomimesis in Drug Delivery: Molecular Imprinting of Biologically Significant Molecules. *Adv. Drug Delivery Rev.* **2004**, *56*, 1599−1620.

(3) Fairlie, D. P.; Tyndall, J. D. A.; Reid, R. C.; Wong, A. K.; Abbenante, G.; Scanlon, M. J.; March, D. R.; Bergman, D. A.; Chai, C. L. L.; Burkett, B. A. Conformational Selection of Inhibitors and Substrates by Proteolytic Enzymes: Implications for Drug Design and Polypeptide Processing. *J. Med. Chem.* **2000**, *43*, 1271−1281.

(4) Luy, B.; Frank, A.; Kessler, H. *Molecular Drug Properties. Measurement and Prediction*; Mannhold, R., Ed.; Wiley-VCH Verlag: Weinheim, Germany, 2008; Chapter 9, pp 207−245.
(5) Lipsitz, R. S.; Tjandra, N. Residual Dipolar Couplings in NMR Structure Analysis. *Annu. Rev. Biophys. Biomol. Struct.* **2004**, *33*, 387−413.
(6) de Alba, E.; Tjandra, N. NMR Dipolar Couplings for the Structure Determination of Biopolymers in Solution. *Prog. Nucl. Magn. Reson. Spectrosc.* **2002**, *40*, 175−197.
(7) Prestegard, J. H.; Al-Hashimi, H. M.; Tolman, J. R. NMR Structures of Biomolecules Using Field Oriented Media and Residual Dipolar Couplings. *Q. Rev. Biophys.* **2000**, *33*, 371−424.
(8) Emsley, J. W. Liquid Crystalline Samples: Structure of Nonrigid Molecules. *Encyclopedia of Magnetic Resonance*; John Wiley & Sons: New York, 2007.
(9) *NMR of Ordered Liquids*; Burnell, E. E.; de Lange, C. A., Eds.; Kluwer Academic: Dordrecht, The Netherlands, 2003.
(10) *Nuclear Magnetic Resonance of Liquid Crystals*; Emsley, J. W., Ed.; Reidel: Dordrecht, The Netherlands, 1985.
(11) Celebre, G.; De Luca, G.; Di Pietro, M. E. Conformational Distribution of *trans*-Stilbene in Solution Investigated by Liquid Crystal NMR Spectroscopy and Compared with *in Vacuo* Theoretical Predictions. *J. Phys. Chem. B* **2012**, *116*, 2876−2885.
(12) Celebre, G.; De Luca, G.; Di Pietro, M. E. The Stable Conformations of 4,4′-Dichloro-*trans*-stilbene in Solution by Liquid Crystal NMR Spectroscopy. *J. Mol. Struct.* **2013**, *1034*, 283−288.
(13) Celebre, G.; Concistré, M.; De Luca, G.; Longeri, M.; Pileio, G.; Emsley, J. W. The Structure of Acrolein in a Liquid Crystal Phase. *Chem.—Eur. J.* **2005**, *11*, 3599−3608.
(14) Concistré, M.; De Lorenzo, L.; De Luca, G.; Longeri, M.; Pileio, G.; Raos, G. Conformational Analysis of 2,2′-Bithiophene: A ^{1}H Liquid Crystal NMR Study Using the ^{13}C Satellite Spectra. *J. Phys. Chem. A* **2005**, *109*, 9953−9963.
(15) Emsley, J. W.; De Luca, G.; Celebre, G.; Longeri, M. The Conformation of the Aromatic Rings Relative to the Alkyl Chain in 4-*n*-Pentyl-4′-cyanobiphenyl. *Liq. Cryst.* **1996**, *20*, 569−575.
(16) Celebre, G.; De Luca, G.; Longeri, M.; Pileio, G.; Emsley, J. W. Is Styrene Planar in Liquid Phases? *J. Chem. Phys.* **2004**, *120*, 7075−7084.
(17) Thiele, C. M.; Schmidts, V.; Böttcher, B.; Louzao, I.; Berger, R.; Maliniak, A.; Stevensson, B. On the Treatment of Conformational Flexibility when Using Residual Dipolar Couplings for Structure Determination. *Angew. Chem., Int. Ed.* **2009**, *48*, 6708−6712.
(18) Kummerlöwe, G.; Luy, B. Residual Dipolar Couplings as a Tool in Determining the Structure of Organic Molecules. *Trends Anal. Chem.* **2009**, *28*, 483−493.
(19) Thiele, C. M. Residual Dipolar Couplings (RDCs) in Organic Structure Determination. *Eur. J. Org. Chem.* **2008**, 5673−5685.
(20) Bax, A.; Grishaev, A. Weak Alignment NMR: A Hawk-eyed View of Biomolecular Structure. *Curr. Opin. Struct. Biol.* **2005**, *15*, 563−570.
(21) Gschwind, R. M. Residual Dipolar Couplings—A Valuable NMR Parameter for Small Organic Molecules. *Angew. Chem., Int. Ed.* **2005**, *44*, 4666−4668.
(22) Aroulanda, C.; Boucard, V.; Guibé, F.; Courtieu, J.; Merlet, D. Weakly Oriented Liquid-Crystal NMR Solvents as a General Tool to Determine Relative Configurations. *Chem.—Eur. J.* **2003**, *9*, 4536−4539.
(23) Samulski, E. T.; Tobolski, A. V. Some Unusual Properties of Poly(γ-benzyl L-glutamate) Films Cast in Strong Magnetic Fields. *Macromolecules* **1968**, *1*, 555−557.
(24) Marx, A.; Böttcher, B.; Thiele, C. M. Enhancing the Orienting Properties of Poly(γ-benzyl-L-glutamate) by Means of Additives. *Chem.—Eur. J.* **2010**, *16*, 1656−1663.
(25) Aroulanda, C.; Lafon, O.; Lesot, P. Enantiodiscrimination of Flexible Cyclic Solutes Using NMR Spectroscopy in Polypeptide Chiral Mesophases: Investigation of *cis*-Decalin and THF. *J. Phys. Chem. B* **2009**, *113*, 10628−10640.
(26) Lesot, P.; Sarfati, M.; Courtieu, J. Natural Abundance Deuterium NMR Spectroscopy in Polypeptide Liquid Crystals as a New and Incisive Means for Enantiodifferentiation of Chiral Hydrocarbons. *Chem.—Eur. J.* **2003**, *9*, 1724−1745.
(27) O' Hagan, D.; Goss, R. J. M.; Meddour, A.; Courtieu, J. Assay for Enantiomeric Analysis of [2H1]-Fluoroacetic Acid: Insight into the Stereochemical Course of Fluorination During Fluorometabolite Biosynthesis in Streptomyces cattleya. *J. Am. Chem. Soc.* **2003**, *125*, 379−387.
(28) Thiele, C. M.; Berger, S. Probing the Diastereotopicity of Methylene Protons in Strychnine Using Residual Dipolar Couplings. *Org. Lett.* **2003**, *5*, 705−708.
(29) Aroulanda, C.; Boucard, V.; Guibé, F.; Courtieu, J.; Merlet, D. Weakly Oriented Liquid-Crystal NMR Solvents as a General Tool to Determine Relative Configurations. *Chem.—Eur. J.* **2003**, *9*, 4536−4539.
(30) Rivard, M.; Guillen, F.; Fiaud, J.-C.; Aroulanda, C.; Lesot, P. Efficient Enantiodiscrimination of Chiral Monophosphine Oxides and Boranes by Phosphorus Coupled ^{13}C NMR Spectroscopy in the Presence of Chiral Ordering Agents. *Tetrahedron: Asymmetry* **2003**, *14*, 1141−1152.
(31) Courtieu, J.; Lesot, P.; Meddour, A.; Merlet, D.; Aroulanda, C. Chiral Liquid Crystal NMR: A Tool for Enantiomeric Analysis. *Encycl. NMR: Adv. NMR* **2002**, *9*, 497−505.
(32) Villar, H.; Guibé, F.; Aroulanda, C.; Lesot, P. Investigation of SmI_2 Mediated Cyclisation of δ-Iodio-α,β-unsaturated Esters by Deuterium 2D NMR in Oriented Solvents. *Tetrahedron: Asymmetry* **2002**, *13*, 1465−1475.
(33) Aroulanda, C.; Sarfati, M.; Courtieu, J.; Lesot, P. Investigation of the Enantioselectivity of Three Polypeptide Liquid-Crystalline Solvents Using NMR Spectroscopy. *Enantiomer* **2001**, *6*, 281−287.
(34) Canlet, C.; Merlet, D.; Lesot, P.; Meddour, A.; Loewenstein, A.; Courtieu, J. Deuterium NMR Stereochemical Analysis of *Threo-erythro* Isomers Bearing Remote Stereogenic Centres in Racemic and Non-racemic Liquid Crystalline Solvents. *Tetrahedron: Asymmetry* **2000**, *11*, 1911−1918.
(35) Fountoulaki, S.; Perdih, F.; Turel, I.; Kessissoglou, D. P.; Psomas, G. Non-steroidal Anti-inflammatory Drug Diflunisal Interacting with Cu(II). Structure and Biological Features. *J. Inorg. Biochem.* **2011**, *105*, 1645−1655.
(36) Pham, T. N.; Watson, S. A.; Edwards, A. J.; Chavda, M.; Clawson, J. S.; Strohmeier, M.; Vogt, F. G. Analysis of Amorphous Solid Dispersions Using 2D Solid-State NMR and ^{1}H T_1 Relaxation Measurements. *Mol. Pharmacol.* **2010**, *7*, 1667−1691.
(37) Ghuman, J.; Zunszain, P. A.; Petitpas, I.; Bhattacharya, A. A.; Otagiri, M.; Curry, S. Structural Basis of the Drug-Binding Specificity of Human Serum Albumin. *J. Mol. Biol.* **2005**, *353*, 38−52.
(38) Brittain, H. G.; Elder, B. J.; Isbester, P. K.; Salerno, A. H. Solid-State Fluorescence Studies of Some Polymorphs of Diflunisal. *Pharm. Res.* **2005**, *22*, 999−1006.
(39) Adamski-Werner, S. L.; Palaninathan, S. K.; Sacchettini, J. C.; Kelly, J. W. Diflunisal Analogues Stabilize the Native State of Transthyretin. Potent Inhibition of Amyloidogenesis. *J. Med. Chem.* **2004**, *47*, 355−374.
(40) Cross, W. I.; Blagden, N.; Davey, R. J. A Whole Output Strategy for Polymorph Screening: Combining Crystal Structure Prediction, Graph Set Analysis, and Targeted Crystallization Experiments in the Case of Diflunisal. *Cryst. Growth Des.* **2003**, *3*, 151−158.
(41) Mao, H.; Hajduk, P. J.; Craig, R.; Bell, R.; Borre, T.; Fesik, S. W. Rational Design of Diflunisal Analogues with Reduced Affinity for Human Serum Albumin. *J. Am. Chem. Soc.* **2001**, *123*, 10429−10435.
(42) Merle, C.; Kummerlöwe, G.; Freudenberger, J. C.; Halbach, F.; Stöwer, W.; Lierse, V.; Gostomski, C.; Höpfner, J.; Beskers, T.; Wilhelm, M.; Luy, B. Crosslinked Poly(ethylene oxide) as a Versatile Alignment Medium for the Measurement of Residual Anisotropic NMR Parameters. *Angew. Chem., Int. Ed.* **2013**, *52*, 10309−10312.
(43) Kummerlöwe, G.; McCord, E. F.; Cheatham, S. F.; Niss, S.; Schnell, R. W.; Luy, B. Tunable Alignment for All Polymer Gel/

Solvent Combinations for the Measurement of Anisotropic NMR Parameters. *Chem.—Eur. J.* **2010**, *16*, 7087−7089.
(44) Kummerlöwe, G.; Udaya Kiran, M.; Luy, B. Covalently Cross-Linked Gelatin Allows Chiral Distinction at Elevated Temperatures and in DMSO. *Chem.—Eur. J.* **2009**, *15*, 12192−12195.
(45) Kummerlöwe, G.; Halbach, F.; Laufer, B.; Luy, B. Precise Measurement of RDCs in Water and DMSO Based Gels Using a Silicone Rubber Tube for Tunable Stretching. *Open Spectrosc. J.* **2008**, *2*, 29−33.
(46) Kummerlöwe, G.; Auernheimer, J.; Lendlein, A.; Luy, B. Stretched Poly(acrylonitrile) as a Scalable Alignment Medium for DMSO. *J. Am. Chem. Soc.* **2007**, *129*, 6080−6081.
(47) Thiele, C. M. Use of RDCs in Rigid Organic Compounds and Some Practical Considerations Concerning Alignment Media. *Concepts Magn. Reson.* **2007**, *30A*, 65−80.
(48) Freudenberger, J. C.; Knör, S.; Kobzar, K.; Heckmann, D.; Paululat, T.; Kessler, H.; Luy, B. Stretched Poly(vinyl acetate) Gels as NMR Alignment Media for the Measurement of Residual Dipolar Couplings in Polar Organic Solvents. *Angew. Chem., Int. Ed.* **2005**, *44*, 423−426.
(49) Luy, B.; Kobzar, K.; Knör, S.; Furrer, J.; Heckmann, D.; Kessler, H. Orientational Properties of Stretched Polystyrene Gels in Organic Solvents and the Suppression of Their Residual ^{1}H NMR Signals. *J. Am. Chem. Soc.* **2005**, *127*, 6459−6465.
(50) Luy, B.; Kobzar, K.; Kessler, H. An Easy and Scalable Method for the Partial Alignment of Organic Molecules for Measuring Residual Dipolar Couplings. *Angew. Chem., Int. Ed.* **2004**, *43*, 1092−1094.
(51) Freudenberger, J. C.; Spiteller, P.; Bauer, R.; Kessler, H.; Luy, B. Stretched Poly(dimethylsiloxane) Gels as NMR Alignment Media for Apolar and Weakly Polar Organic Solvents: An Ideal Tool for Measuring RDCs at Low Molecular Concentrations. *J. Am. Chem. Soc.* **2004**, *126*, 14690−14691.
(52) Emsley, J. W.; Luckhurst, G. R.; Stockley, C. P. A Theory of Orientational Ordering in Uniaxial Liquid Crystals Composed of Molecules with Alkyl Chains. *Proc. R. Soc. London, Ser. A* **1982**, *381*, 117−138.
(53) Celebre, G.; De Luca, G.; Emsley, J. W.; Foord, E. K.; Longeri, M.; Lucchesini, F.; Pileio, G. The Conformational Distribution in Diphenylmethane Determined by Nuclear Magnetic Resonance Spectroscopy of a Sample Dissolved in a Nematic Liquid Crystalline Solvent. *J. Chem. Phys.* **2003**, *118*, 6417−6426.
(54) Müller, K.; Faeh, C.; Diederich, F. Fluorine in Pharmaceuticals: Looking Beyond Intuition. *Science* **2007**, *317*, 1881−1886.
(55) Bégué, J. P.; Bonnet-Delpon, D. Recent Advances (1995−2005) in Fluorinated Pharmaceuticals Based on Natural Products. *J. Fluorine Chem.* **2006**, *127*, 992−1012.
(56) Kirk, K. L. Selective Fluorination in Drug Design and Development: an Overview of Biochemical Rationales. *Curr. Top. Med. Chem.* **2006**, *6*, 1447−1456.
(57) Kirsch, P. *Modern Fluoroorganic Chemistry*; Wiley-VCH Verlag: Weinheim, Germany, 2004; Chapter 4, pp 237−271.
(58) Kirk, K. L. Fluorine in Medicinal Chemistry: Recent Therapeutic Applications of Fluorinated Small Molecules. *J. Fluorine Chem.* **2006**, *127*, 1013−1029.
(59) *Organofluorine Chemistry. Principles and Commercial Applications*; Banks, R. E.; Smart, B. E.; Tatlow, J. C., Eds.; Plenum Press: New York, 1994.
(60) Reichenbächer, K.; Süss, H. I.; Hulliger, J. Fluorine in Crystal Engineering—"The Little Atom That Could". *Chem. Soc. Rev.* **2005**, *34*, 22−30.
(61) Kirsch, P. *Modern Fluoroorganic Chemistry*; Wiley-VCH Verlag: Weinheim, Germany, 2004: Chapter 1, pp 8−16.
(62) Fäcke, T.; Berger, S. SERF, A New Method for H,H Spin-coupling Measurement in Organic Chemistry. *J. Magn. Reson., Ser. A* **1995**, *113*, 114−116.
(63) Di Pietro, M. E.; Aroulanda, C.; Merlet, D. GET-SERF, a New Gradient Encoded SERF Experiment for the Trivial Edition of ^{1}H−^{19}F Couplings. *J. Magn. Reson.* **2013**, *234*, 101−105.
(64) Sarfati, M.; Lesot, P.; Merlet, D.; Courtieu, J. Theoretical and Experimental Aspects of Enantiomeric Differentiation Using Natural Abundance Multinuclear NMR Spectroscopy in Chiral Polypeptide Liquid Crystals. *Chem. Commun. (Cambridge, U. K.)* **2000**, 2069−2081.
(65) Meddour, A.; Berdagué, P.; Hedli, A.; Courtieu, J.; Lesot, P. Proton-Decoupled Carbon-13 NMR Spectroscopy in a Lyotropic Chiral Nematic Solvent as an Analytical Tool for the Measurement of the Enantiomeric Excess. *J. Am. Chem. Soc.* **1997**, *119*, 4502−4508.
(66) Lesot, P.; Merlet, D.; Meddour, A.; Loewenstein, A.; Courtieu, J. Visualization of Enantiomers in a Polypeptide Liquid-Crystal Solvent through Carbon-13 NMR Spectroscopy. *J. Chem. Soc., Faraday Trans.* **1995**, *91*, 1371−1375.
(67) Kalinowski, H. O.; Berger, S.; Braun, S. *Carbon-13 NMR Spectroscopy*; John Wiley & Sons: Chichester, U.K., 1988.
(68) Emsley, J. W.; Lesot, P.; De Luca, G.; Lesage, A.; Merlet, D.; Pileio, G. A Comparison of Proton-Detected ^{13}C Local Field Experiments with Deuterium NMR at Natural Abundance for Studying Liquid Crystals. *Liq. Cryst.* **2008**, *35*, 443−464.
(69) Emsley, J. W.; Lesot, P.; Merlet, D. The Orientational Order and Conformational Distributions of the Two Enantiomers in a Racemic Mixture of a Chiral, Flexible Molecule Dissolved in a Chiral Nematic Liquid Crystalline Solvent. *Phys. Chem. Chem. Phys.* **2004**, *6*, 522−530.
(70) Merlet, D.; Ancian, B.; Courtieu, J.; Lesot, P. Two-Dimensional Deuterium NMR Spectroscopy of Chiral Molecules Oriented in a Polypeptide Liquid Crystal: Applications for the Enantiomeric Analysis through Natural Abundance Deuterium NMR. *J. Am. Chem. Soc.* **1999**, *121*, 5249−5258.
(71) Merlet, D.; Ancian, B.; Smadja, W.; Courtieu, J.; Lesot, P. Analysis of Natural Abundance Deuterium NMR Spectra of Enantiomers in Chiral Liquid Crystals *via* 2D Auto-correlation Experiments. *Chem. Commun. (Cambridge, U. K.)* **1998**, 2301−2302.
(72) Emsley, J. W.; Lesot, P.; Lesage, A.; De Luca, G.; Merlet, D.; Pileio, G. The Conformation and Orientational Order of a 1,2-Disubstituted Ethane Nematogenic Molecule (I22) in Liquid Crystalline and Isotropic Phases Studied by NMR Spectroscopy. *Phys. Chem. Chem. Phys.* **2010**, *12*, 2895−2914.
(73) Frisch, M. J.; Trucks, G. W.; Schlegel, H. B.; Scuseria, G. E.; Robb, M. A.; Cheeseman, J. R.; Scalmani, G.; Barone, V.; Mennucci, B.; Petersson, G. A.; et al. *Gaussian 09* (Revision A.02); Gaussian: Wallingford, CT, USA, 2009.
(74) Cossi, M.; Scalmani, G.; Rega, N.; Barone, V. New Developments in the Polarizable Continuum Model for Quantum Mechanical and Classical Calculations on Molecules in Solution. *J. Chem. Phys.* **2002**, *117*, 43−54.
(75) Celebre, G.; De Luca, G.; Longeri, M. Exploiting the Information Content of Dipolar Couplings: Determination of the Temperature Dependence of the Inter-ring Twist Angle of Biphenyl Dissolved in Uniaxial Mesophases. *Liq. Cryst.* **2010**, *37*, 923−933.
(76) Celebre, G.; Longeri, M. *NMR of Ordered Liquids*; Burnell, E. E.; de Lange, C. A, Eds.; Kluwer Academic: Dordrecht, The Netherlands, 2003; Chapter 14, pp 305−324.
(77) Emsley, J. W.; Lesot, P.; Courtieu, J.; Merlet, D. The Effect of a Chiral Nematic Solvent on the Orientational Order and Conformational Distribution of a Flexible Prochiral Solute. *Phys. Chem. Chem. Phys.* **2004**, *6*, 5331−5337.
(78) Pileio, G. Ph.D. Thesis, Università della Calabria, Italy, 2005.
(79) Bondi, A. van der Waals Volumes and Radii. *J. Phys. Chem.* **1964**, *68*, 441−451.
(80) Grein, F. Twist Angles and Rotational Energy Barriers of Biphenyl and Substituted Biphenyls. *J. Phys. Chem. A* **2002**, *106*, 3823−3827.